Available online at www.sciencedirect.com
ScienceDirect
Journal of Hazardous Materials 153 (2008) 566–574
Journal of Hazardous Materials
www.elsevier.com/locate/jhazmat

The removal of the indigo carmine dye from aqueous solutions using cross-linked chitosan—Evaluation of adsorption thermodynamics using a full factorial design

Antonio R. Cestari [a,*], Eunice F.S. Vieira [a], Andréa M.G. Tavares [a], Roy E. Bruns [b]

[a] *Laboratory of Materials and Calorimetry, Departamento de Química/CCET, Universidade Federal de Sergipe, CEP 49100-000, São Cristóvão, Sergipe, Brazil*

[b] *Universidade Estadual de Campinas, Instituto de Química, CP 6154, 13083-970 Campinas, São Paulo, Brazil*

Received 25 April 2007; received in revised form 29 August 2007; accepted 29 August 2007
Available online 4 September 2007

Abstract

A 2^3 factorial design was employed to evaluate the quantitative removal of the indigo carmine (IC) dye from aqueous solutions on glutaraldehyde cross-linked chitosan. The variables were chitosan masses of 100 and 300 mg, IC concentrations of 2.0 and 5.0×10^{-5} mol L^{-1} and temperatures of 25 and 35 °C. The quantitative and energetic adsorption parameters were analyzed statistically using modeling with bilinear equations. The results indicated that increasing the chitosan mass from 100 to 300 mg decreases the IC adsorption/mass ratio (mol g^{-1}) whereas a temperature increase of 25–35 °C increases it. The principal effect of the IC concentration did not show statistical significance. The factorial experiments demonstrate the existence of a significant antagonistic interaction effect between the chitosan mass and temperature.

The adsorption thermodynamic parameters, namely $\Delta_{ads}H$, $\Delta_{ads}G$, and $\Delta_{ads}S$, were determined for all the factorial design results. Endothermic values were found in relation to the $\Delta_{ads}H$. The positive $\Delta_{ads}S$ values indicate that entropy is a driving force for adsorption. The $\Delta_{ads}G$ values are also significantly affected by important antagonistic and synergistic effects involving all principal and interactive factors. It is concluded that the thermodynamical spontaneity of the IC adsorption parameters are greatly influenced by the interactive factors and not by the temperature changes alone.

Keywords: Chitosan; Removal of dyes; Adsorption thermodynamics; Chemometrics

1. Introduction

Chitin is a biodegradable and non-toxic polysaccharide widely spread among marine and terrestrial invertebrates and fungi [1,2]. It is usually obtained from waste materials of the sea food-processing industry, mainly shells of crab, shrimp, prawn and krill. Native chitin occurs in these natural composite materials usually combined with inorganics, proteins, lipids and pigments. Its isolation calls for chemical treatments to eliminate these contaminants [3,4]. By treating crude chitin with aqueous 40–50% sodium hydroxide in the 110–115 °C range chitosan is obtained [5]. Fig. 1 presents a schematic representation of the structures of the partially deacetylated chitosan structure. Both biopolymers are chemically similar to cellulose, differing only from the R group attached to carbon 2 of the general carbohydrate structure. Chitin and chitosan are closely related since both are linear polysaccharides containing 2-acetamido-2-deoxy-D-glucopyranose and 2-amino-2-deoxy-D-glucopyranose units joined by β(1 → 4) glycosidic bonds. Due to the features mentioned, the chemical and physical properties of these polymers are different in nature [6]. The fully deacetylated product is rarely obtained due to the risks of side reactions and chain depolymerization [6].

Applications for chitosan currently are found in industrial wastewater treatment and in recovery of feed grade material from food processing plants [7]. Numerous studies have demonstrated the effectiveness of chitosan and derived products in the uptake of metal cations such as lead, cadmium, copper, and nickel and the uptake of oxyanions as well complexed metal ions. In other areas, chitosan has been employed as an excellent adsorbent for

* Corresponding author. Tel.: +55 79 32126656; fax: +55 79 32126684.
E-mail address: cestari@ufs.br (A.R. Cestari).

0304-3894/$ – see front matter © 2007 Elsevier B.V. All rights reserved.
doi:10.1016/j.jhazmat.2007.08.092

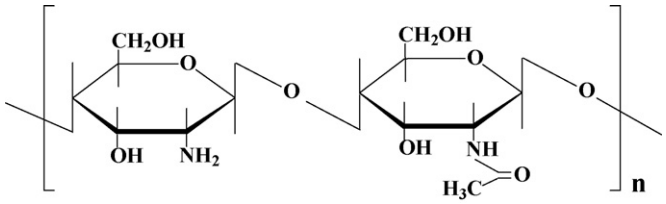

Fig. 1. Structures of partially deacetylated chitosan.

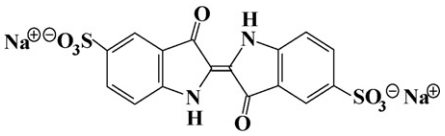

Fig. 2. Chemical structure of indigo carmine dye (IC).

sorption of phenols and polychlorined biphenyls [8], anionic dyes [9], enzymes [10], and in pollution control, as a chelating polymer for binding harmful metal ions [11].

The extent of metal and/or dye adsorption depends on the source of chitosan, the degree of deacetylation, the nature of the adsorbate molecules, and solution conditions such as the solvent and the adsorption pH value, which makes experimental procedures the only manner to evaluate the interactive chitosan-adsorbate molecule. Since these studies involve a prohibitively large number of experiments, chemometric procedures based on multivariate statistical techniques are employed here. Statistical methods of experimental design and system optimization such as factorial design and response surface analysis have been applied to different adsorption systems because of their capacities to extract relevant information from systems while requiring a minimum number of experiments. Examples of recent applications of the factorial design methodology in adsorption from solution are found, for instance, in the interaction of non-ionic dispersant on lignite particles [12], removal of Ga(III) from aqueous solution using bentonite [13], adsorption of cationic dye on activated carbon beads [14], and optimization of solid-phase extraction and separation of metabolites using HPLC [15]. Since, substantial interactions among the experimental adsorption variables are frequently evidenced, which can predominate over main factor effects, univariate optimization strategies have been shown to be relatively inadequate in these kinds of adsorption studies. Besides economizing experimental effort, multivariate methods are capable of measuring interaction effects on metal adsorption as well as the individual effect of each experimental factor on response properties of interest in the most precise way possible. However, to our knowledge, despite the large number of works concerning adsorption of metals and dyes on chitosan, the role of experimental parameter changes on the thermodynamic of adsorption, such as temperature, amount of chitosan and solute concentration, as well as their interactions, are few and scattered.

In this work, chitosan was cross-linked to improve the chemical and mechanical features of raw chitosan. A 2^3 complete factorial design was used to evaluate the importance of three experimental factors concerning the adsorption quantities and the thermodynamical adsorption of the anionic dye indigo carmine on cross-linked chitosan. The factorial design required the execution of a relatively small number of different experiments. To determine the statistical significance of the effects, duplicate determinations were made for each of these experiments to evaluate experimental error.

2. Materials and methods

2.1. Materials and preliminary characterization of the raw chitosan sample

Water was used after double-distillation. The indigo carmine dye (disodium salt of 3,3-dioxobi-indolin-2,2-ylidine-5,5-disulfonate, abbreviated as IC, Merck), whose chemical structure is shown in Fig. 2, was used as-received.

The chitosan powder used was from fresh Norwegian shrimp shells from Primex Ingredients A.S. (Norway/Iceland). The following characterizations were performed (details not shown), in order to check some important aspects, concerning the purity and structural aspects of the chitosan sample. Briefly, the degree of deacetylation was determined by infrared spectroscopy [16]. Solid-state ^{13}C NMR spectroscopy was used to verify the purity of the chitosan sample by the positions and their respective intensities of the ^{13}C absorption peaks, from 20 to 200 ppm [11,16]. The total quantity of nitrogen was determined by the Kjeldhal method.

The raw chitosan powder was cross-linked using a 2% (m/v) glutaraldehyde (VETEC/Brazil) solution as described earlier [1]. Fig. 3 shows a schematic view of the glutaraldehyde-modified chitosan cross-linking reaction. The cross-linked chitosan was sieved and used in the 60–100 mesh range and conditioned in a dark air-free flask, in order to prevent possible interactions between the amine groups and atmospheric CO_2 [17].

The thermogravimetric analyses (TG and DTG) were made using about 10 mg of material, under nitrogen atmosphere from 25 to 600 °C, in a SDT 2960 thermoanalyzer, from TA Instruments. The X-ray analyses were performed with a Rigaku diffractometer, in the 2θ range from 5° to 80° (accumulation rate of 0.02 min^{-1}).

2.2. Adsorption experiments

A full 2^3 factorial design was performed to evaluate the importance of the chitosan mass, the IC dye concentration and temperature on the quantity of dye adsorbed. Table 1 summarizes these factors and their respective levels. The adsorptions of

Table 1
Factors and levels used in the 2^3 factorial design study

Factors	Levels	
	(−)	(+)
Quantity of chitosan, Q (mg)	100	300
Concentration of dye, C ($\times 10^{-5}$ mol L^{-1})	2.0	5.0
Temperature, T (°C)	25	35

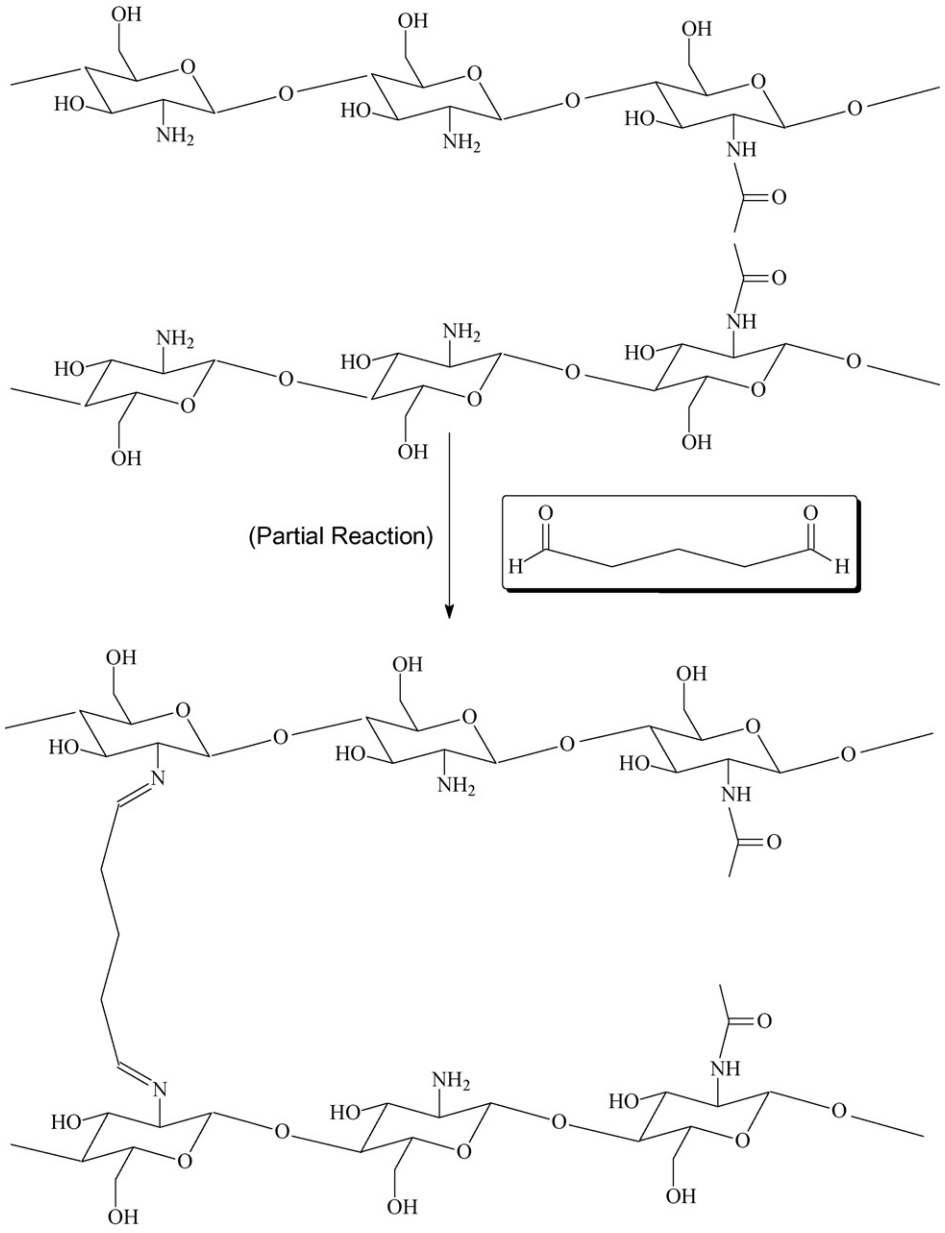

Fig. 3. Partial cross-linking reaction of chitosan using glutaraldehyde. Experimental details: 2% (m/v) of glutaraldehyde aqueous solution; stirring time, 3 h; room temperature, 25 °C.

the IC dye were performed using a batch procedure [18], where 50 mL of the IC solutions were agitated for 200 min, sufficient time to reach equilibrium, according to the kinetic isotherms results (Fig. 4), which were performed using the same experimental conditions of each factorial design experiment. In order to increase the IC removal and to preserve the polymeric chemical structure of the chitosan, the pH values of the solutions were adjusted to 4.0 using a 0.1 mol L^{-1} HCl solution. After a predetermined contact time, supernatant aliquots were separated by decantation and the IC dye concentrations were determined spectrophotometrically at 555 nm.

The adsorptions of IC dye were calculated using the expression [9,18]:

$$N_f = \frac{(C_i - C_e)V}{m} \quad (1)$$

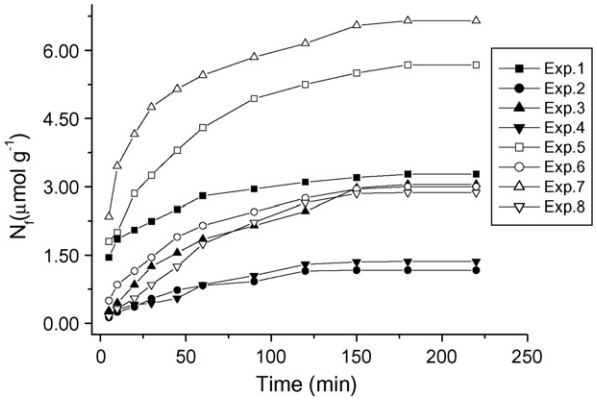

Fig. 4. Kinetic isotherms of the adsorption of the IC dye into the cross-linked chitosan at the same conditions of the factorial design matrix (Table 3).

Table 2
Adsorption results[a] (N_f, upper table) and the Gibbs free energies ($-\Delta_{ads}G$, lower table) of the 2^3 factorial design for the interactions of IC with chitosan

Experiment	Q	C	T	$N_f(1)$ (μmol g^{-1})	$N_f(2)$ (μmol g^{-1})	$N_f(m)$ (μmol g^{-1})	$N_f(p)$[b] (μmol g^{-1})
1	−1	−1	−1	3.56	2.99	3.27	3.16
2	1	−1	−1	1.13	1.20	1.17	1.26
3	−1	1	−1	3.01	3.09	3.05	3.16
4	1	1	−1	1.43	1.29	1.36	1.26
5	−1	−1	1	5.93	5.44	5.68	6.16
6	1	−1	1	2.98	3.03	3.00	2.94
7	−1	1	1	6.39	6.91	6.65	6.16
8	1	1	1	2.94	2.80	2.87	2.94

Experiment	Q	C	T	$-\Delta_{ads}G$ (1) (kJ mol^{-1})	$-\Delta_{ads}G$ (2) (kJ mol^{-1})	$-\Delta_{ads}G$ (m) (kJ mol^{-1})	$-\Delta_{ads}G$ (p)[b] (kJ mol^{-1})
1	−1	−1	−1	11.13	10.49	10.81	10.79
2	1	−1	−1	8.22	8.45	8.33	8.33
3	−1	1	−1	7.67	7.74	7.71	7.71
4	1	1	−1	5.97	5.67	5.82	5.81
5	−1	−1	1	14.44	13.91	14.17	14.17
6	1	−1	1	16.17	16.62	16.40	16.39
7	−1	1	1	10.62	10.90	10.76	10.77
8	1	1	1	8.93	8.74	8.83	8.83

[a] N_f (1), N_f (2), $-\Delta_{ads}G$ (1) and $-\Delta_{ads}G$ (2) represent duplicate values, under the same experimental conditions. N_f (m) and $-\Delta_{ads}G$ (m) values are the respective averages.
[b] N_f (p) and $-\Delta_{ads}G$ (p) represent the average adsorption results predicted from Eq. (4) (N_f) and Eq. (11) ($\Delta_{ads}G$).

where N_f is the fixed quantity of dye per gram of chitosan at a given time t (mol/g), C_i the initial concentration of dye (mol/L), C_e the concentration of dye present at a given time t (mol/L), V the volume of the solution (L), and m is the mass of chitosan (g). Table 2 presents the quantities of moles of dye absorbed for each factorial experiment.

The statistical calculations (t-tests, F-tests, analysis of variance (ANOVA) and multiple regressions) were performed using the ORIGIN®, release 6.0, software and the Statistica® software packages [19].

3. Results and discussion

3.1. Initial considerations

The amount of nitrogen of the chitosan, before and after the cross-linking reaction, showed the presence of $6.77 \pm 0.30\%$ (4.84 ± 0.25 mmol g) and $6.50 \pm 0.34\%$ (4.42 ± 0.25 mmol g) of nitrogen. The TG and DTG curves of the cross-linked chitosan are shown in Fig. 5. The first mass loss step, from about 25 to 220 °C concerns the loss of water, which is adsorbed on both the surface and the pores of chitosan [20]. The decomposition of the chitosan structure is observed from about 220 to 420 °C. It can be observed that the profiles of the TG/DTG curves, for both non-cross-linked and cross-linked materials, are very similar.

The XRD diffractograms of the non-cross-linked and cross-linked chitosan are show in Fig. 6. The presence of a main peak at about $2\theta = 21°$ was observed in both diffractograms. Other small peaks are relatively similar to one another in relation to their positions and intensities.

The characterizations of the materials using TG/DTG, XRD and BET surface areas (10.0 and 8.0 m^2 g^{-1}, before and after the cross-linking reactions, respectively) suggest that structural characteristics of the materials are retained after the cross-linking reaction.

Adsorptions of metals from solutions take place using typically both immobilized nitrogenated and oxygenated Lewis bases of the chitosan structure [1,3]. On the other hand, adsorptions of anionic dyes occur mainly due to the electrostatic interactions between the protonated amine groups on the chitosan ($-NH_3^+$) and the SO_3^- groups of the anionic dyes structures [21].

3.2. Factorial designs calculations

3.2.1. Calculation and analysis of the adsorption factors

The adsorbate concentration, pH, temperature and other experimental factors, have been shown to be significant in the adsorption of dyes taking into account their environmental impact, at dye trace levels [22]. Note that the factors used in this work have never been investigated simultaneously using

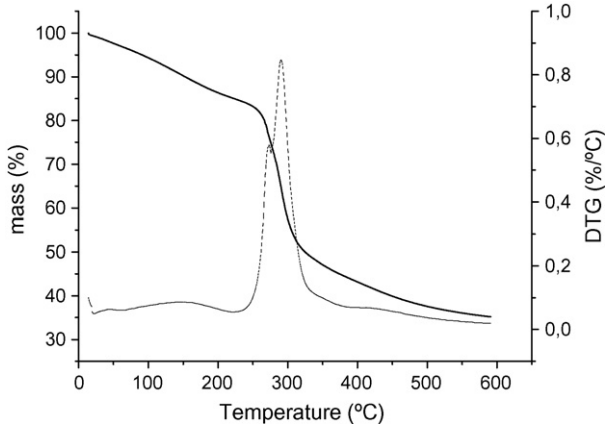

Fig. 5. TG (full) and DTG (dashed) curves of the cross-linked chitosan.

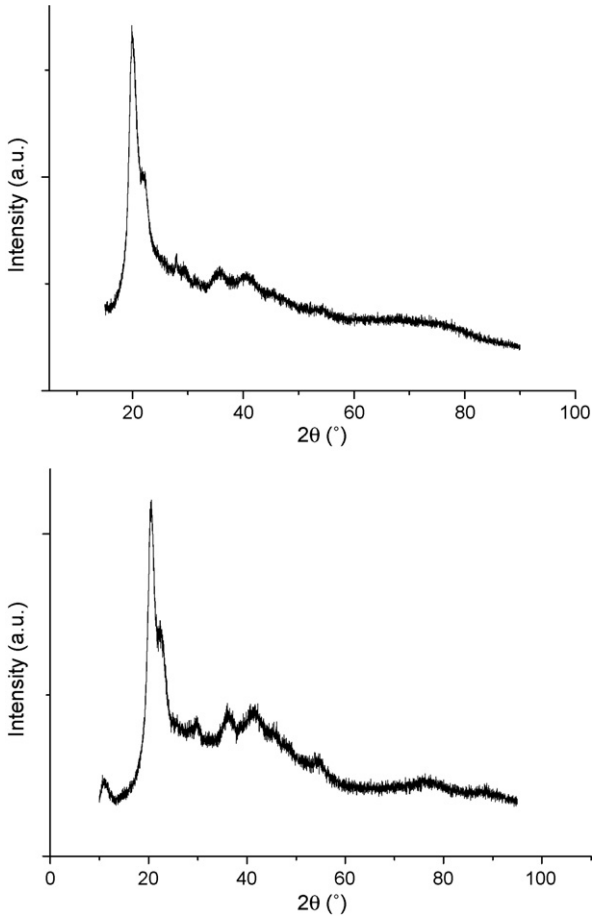

Fig. 6. X-ray diffractograms of the non-cross-linked (upper) and cross-linked chitosan (lower).

factorial designs, and they were chosen for their importance, as determined previously using one-variable-at-a-time experimental procedures [1]. The experiments were executed in random order to correctly evaluate experimental errors [23].

Principal and interaction effect values are easily calculated from factorial design results. Both types of effects are calculated using the following equation [23]:

$$\text{effect} = \bar{R}_{+,i} - \bar{R}_{-,i} \quad (2)$$

where $\overline{R}_{+,i}$ and $\overline{R}_{-,i}$ are average values of N_f for the high (+) and low (−) levels of each factor. For principal or main effects the above averages simply refer to the results at the high (+) and low (−) levels of the factor whose effect is being calculated independent of the levels of the other factors. For binary interactions $\bar{R}_+$ is the average of results for both factors at their high and low levels whereas $\overline{R}_-$ is the average of the results for which, one of the factors involved is at the high level and the other is at the low level. In general, high-order interactions are calculated using the above equation by applying signs obtained by multiplying those for the factors involved (+) for high and (−) for low levels. If duplicate runs are performed for each individual measurement, as done in this work, standard errors (S.E.) in the effect values can be calculated by [23,24]:

$$E = \left\{ \frac{\sum (d_i)^2}{8N} \right\}^{1/2} \quad (3)$$

where d_i is the difference between each duplicate value and N is the number of distinct experiments performed.

The results obtained in a factorial design depend, in part, on the ranges of the factors studied. The chosen levels should be large enough to provoke response changes that are larger than experimental error. However, these differences should not be so large that quadratic or higher order effects due to the individual factors become important and invalidate the factorial model. Under these conditions factorial designs are particularly efficient for evaluating the principal effects of each factor and their interactions on the metal adsorptions as well as those for academic and industrial processes [25].

The factorial design results are in Table 2 and the respective principal and interaction effects for the first factorial design study are presented in Table 3. On average, a decrease in the chitosan mass causes an increase in the degree of adsorption observed. This is indicated by the principal effect for chitosan mass of -2.56×10^{-6} mol g^{-1}. A similar behavior of the "mass effect" was also detected earlier [25,26]. When both the initial concentrations of dye and the volume of the solutions remain unchanged, an increase in adsorbent mass in solution was found to decrease the probability for the reaction between the active sites of adsorbent and the dye in solution. Consequently, the adsorption/mass ratios (mol g^{-1}) of solute (IC dye in the present work) decrease [26].

On the other hand, increasing the IC concentration factor did not affect adsorption in relation to the N_f values in the factorial experiment. Indeed, the quantitative adsorption, in one-variable-at-time methodology, is significantly changed when the initial dye concentrations are very different one another [27].

The adsorption increased for the higher temperature value in the factorial design. So, the "temperature effect" in this factorial design is also an important factor for the removal of anionic dyes using chitosan. A similar "temperature effect" was also observed in our paper published earlier, on the determination of the thermochemical parameters of the IC–chitosan interaction using the so-called one-variable-at-time methodology [27].

Table 3
Effect values and their standard errors for the interactions of the IC dye with the cross-linked chitosan

Effects	N_f (μmol g^{-1})	$\Delta_{ads}G$ (kJ mol^{-1})
Average	3.38 ± 0.06	−10.35 ± 0.06
Principal		
Q	−2.56 ± 0.12	1.02 ± 0.13
C	0.20 ± 0.12	4.15 ± 0.13
T	2.34 ± 0.12	−4.38 ± 0.13
Interactions		
Q–C	−0.17 ± 0.12	0.89 ± 0.13
Q–T	−0.67 ± 0.12	−1.16 ± 0.13
C–T	0.22 ± 0.12	1.34 ± 0.13
Q–C–T	−0.38 ± 0.12	1.18 ± 0.13

The interaction effect absolute values are much smaller than the chitosan mass and temperature main effects. However, at the 95% confidence level, the interaction effect between chitosan mass and temperature is statistically important. The effect will be seen to be important for obtaining a quantitative model for this chitosan adsorption process.

3.2.2. Modeling of the quantitative adsorption of IC dye on the cross-linked chitosan

A quantitative model for the amounts of absorbed IC dye can be written in terms of the statistically significant effects on N_f in Table 3 [23,24]:

$$N_f = 3.38 - 1.28x_1 + 1.17x_3 - 0.33x_1x_3 \quad (4)$$

where x_1 and x_3 are codified (± 1) values of chitosan quantity and temperature.

The predicted adsorption values ($N_f(p)$), are presented in the upper part of Table 2. The agreement between these values is quite good with a root mean square error of 0.26 μmol g^{-1}. If the interaction term is left out of the model the error increases significantly to 0.41 μmol g^{-1}.

In Eq. (4), the model predicts the dependence of the amount of adsorbed IC dye using chitosan masses of 100 or 300 mg in contact with the IC dye solution at 25 or 35 °C. This is a consequence of the fact that no effect involving the dye concentration was found. Note that the chitosan amount effect is negative and very similar in value to the one found for the metal–chitosan interaction study reported earlier [25]. Increasing the chitosan amount from 100 to 300 mg decreases the quantity of IC dye adsorbed by $2 \times (1.28) \times 10^{-6} = 2.56 \times 10^{-6}$ mol g^{-1}. Increasing the temperature from 25 to 35 °C, on the other hand, increases the IC dye adsorbed by $2 \times (1.17) \times 10^{-6} = 2.34 \times 10^{-6}$ mol g^{-1}.

Since there are no important effects involving the concentration of dye used in the experiments, the adsorption process just depends on the chitosan amount-temperature levels for the experimental domain investigated here. Fig. 7 gives a detailed description of the amount of dye adsorbed as a function of chitosan mass and temperature. The quantities of adsorbed dye given at the vertices are averages of all the experimental results for the temperature and chitosan mass conditions shown in the figure. Note that the effect of a temperature increase from 25 to 35 °C is twice as large (+3.01 μmol g^{-1}) for a 2.0×10^{-5} mol L^{-1} dye solution than for a 5.0×10^{-5} mol L^{-1} one (+1.67 μmol g^{-1}). This behavior can also be explained using chitosan mass effects at the two temperatures. The effect of increasing the chitosan mass from 100 to 300 mg at 35 °C results in a decrease in the quantity of adsorbed dye of -3.23×10^{-6} mol g^{-1} that is twice as large as the one observed at 25 °C, -1.89×10^{-6} mol g^{-1}. This rather complex behavior is neatly described by the significant chitosan mass–temperature interaction effect of -0.67×10^{-6} mol g^{-1} given in Table 3.

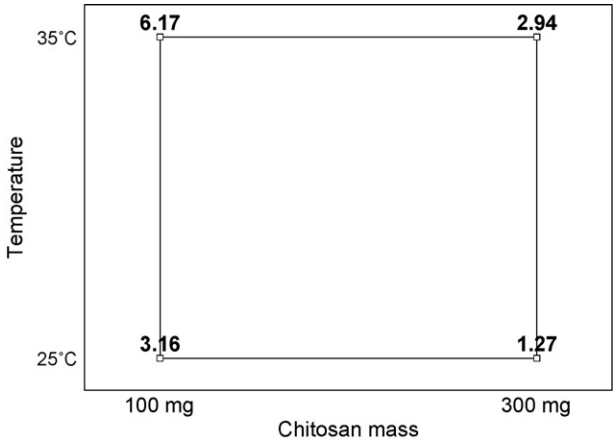

Fig. 7. The quantities of dye adsorbed in μmol g^{-1} for the investigated chitosan mass and temperature levels.

Taking into account that it is the first attempt to study adsorption of an anionic dye on chitosan simultaneously using all these factors, further statistical studies will point out a more accurate modeling to evaluate the relative importance of each experimental factor of the quantitative anionic dyes adsorptions on chitosan. However, other adsorption parameters, using the factorial design results, can also be calculated and evaluated, as described hereafter.

3.3. Thermodynamic of adsorption of IC dye on the cross-linking chitosan

3.3.1. Determination and analysis of enthalpy, entropy, and Gibbs free energies for the IC dye adsorption according to the factorial design

The thermodynamic parameters, namely the equilibrium constants (K), the enthalpy of adsorption ($\Delta_{ads}H$), the Gibbs free energies of adsorption ($\Delta_{ads}G$) and the entropy of adsorption ($\Delta_{ads}S$) were calculated as shown in Eqs. (5)–(8) [28–30], using the average adsorption quantities of the factorial design matrix, in relation to the following general equilibrium:

$$\text{chitosan–NH}_{2(s)} + \text{dye (eq)}_{(aq)} \text{chitosan–NH}_2\text{/dye}_{(s)}$$

$$K = \frac{\theta}{(1-\theta)C_{eq}} \quad (5)$$

$$\ln\frac{K_{35}}{K_{25}} = \Delta_{ads}H\frac{T_{35}-T_{25}}{R(T_{35}T_{25})} \quad (6)$$

$$\Delta_{ads}G = -RT\ln K \quad (7)$$

$$\Delta_{ads}G = \Delta_{ads}H - T\Delta_{ads}S \quad (8)$$

where θ is the fraction of adsorption that are occupied by IC in relation to the available free NH_2 groups on chitosan after cross-linking reaction, or 3.10 mmol NH_2/chitosan mass. Thus, $\theta = N_f$/(3.10 mmol NH_2/chitosan mass). C_{eq} is the equilibrium concentration (mol L^{-1}) of dye in solution, T the solution temperature (K), which was used in relation to each factorial design and R is the universal gas constant (8.314 J K^{-1} mol^{-1}).

In univariate adsorption studies, the thermodynamic aspects of adsorption are directly related to the changes of the adsorption temperature [31]. However, from the results of the multivariate study found in this work, the effect of the chitosan mass and concentration was also very expressive in relation to the calculated error. So, the different values for the thermodynamic parameters

Table 4
Thermodynamic parameters[a] of the adsorption of IC in relation to the 2^3 factorial design results

Experiment	Var Q	Var C	Var T	ln K	$\Delta_{ads}H$[b] (kJ mol^{-1})	$-\Delta_{ads}G$ (kJ mol^{-1})	$\Delta_{ads}S$ (J K^{-1} mol^{-1})
1	−1	−1	−1	4.37	38.21	10.81	37.4
2	1	−1	−1	3.42	110.33	8.33	27.9
3	−1	1	−1	3.14	36.27	7.71	25.8
4	1	1	−1	2.28	40.10	5.82	20.2
5	−1	−1	1	5.48	38.21	14.17	45.5
6	1	−1	1	6.10	110.33	16.40	51.2
7	−1	1	1	3.97	36.27	10.76	33.5
8	1	1	1	3.38	40.10	8.83	28.2

[a] All thermodynamic values were calculated in relation to the average equilibrium adsorption quantities (N_f (m)).
[b] For small temperature ranges ($\Delta T = 10\,^{\circ}C$, in this work), the $\Delta_{ads}H$ values do not change significantly. See Ref. [32] for details.

of the IC dye adsorption on chitosan can be due to the role of all principal and interactive factors of the factorial design and not to the temperature effect alone [32].

Table 4 shows the calculated values of the thermodynamic parameters for the IC dye adsorptions on the cross-linked chitosan. The equilibrium constants are found to be different from one another, due to the differences in the N_f values found in the factorial design results. The different tendencies of the solvent detachment from both the dye molecule and the interaction sites of the chitosan at 25 or 35 °C, as well as the different modes of interaction of the dye in relation to the adsorbent (chitosan) coverage have been also considered as important factors to produce different adsorption thermodynamic quantities [32,33].

The values of $\Delta_{ads}H$ indicate endothermic adsorption processes for all factorial design experiments. One possible explanation of the endothermicity of heats of adsorption [34,35] is the well-known fact that dyes and carbohydrate materials are both well solvated in water. In order for the dyes to be adsorbed, they have to lose part of their hydration shell. The dehydration processes of the dyes and the adsorbent surface require energy. So, the dehydration processes supersede the exothermicity of the adsorption processes. In summary, we may say that the removal of water from the dyes and the chitosan structure is essentially an endothermic process and it appears that endothermicity of the desolvation processes, in most cases in this study, exceeds that of the exothermicity provided by the heat of adsorption. However, we are unable to point out the extension of these desolvation processes, using the adsorption data of this work. We think that additional computational studies should be useful in the future, in order to estimate the endothermicity of the desolvation processes. The main difficulties are related to understanding the correct fraction of solvent released from both the dye molecules in solution and chitosan at a given temperature. The unreacted hydroxyl groups present on chitosan would also contribute to adsorption and release of water present on the chitosan [1,6]. The involved adsorption steps, at equilibrium conditions, can be stated, in a simplified manner, as follows [32,33]:

$$\text{adsorbent} + \text{solvent} = \text{adsorbent(solvent)} \quad (9)$$

$$\text{adsorbent(solvent)} + \text{dye(solvent)} = \text{adsorbent–dye(solvent)} + \text{solvent} \quad (10)$$

As can be seen from Table 2, the positive values of $\Delta_{ads}H$ indicate the presence of an energy barrier in the adsorption process. The positive $\Delta_{ads}S$ values indicate that entropy is also a driving force for adsorption [36].

Table 5
Comparative values of $\Delta_{ads}H$ (kJ mol^{-1}) for some adsorbent/dye interactions from aqueous solutions

Adsorbent/adsorbate	$\Delta_{int}H$ (kJ mol^{-1})	Reference
Zeolite MCM-22/basic dye	+5.4	[39]
Carbon slurry/ethyl orange	−6.20	[38]
Carbon slurry/chrysoidine B	−0.70	[38]
Fly ash/basic fuchsin	21.4	[38]
Fly ash/methylene blue	76.1	[38]
Red mud/ methylene blue	10.8	[38]
Coir pith/congo red	7.71	[38]
Red mud/methylene blue	−31.0	[38]
Fullers earth/methylene blue	158	[38]
Bentonite/nylosan red EBL	26.8	[40]
Bentonite/ nylosan blue EBL	12.2	[40]
Wool fibers/acid violet 17	20.9	[41]
Wool fibers/acid blue 90	23.3	[41]
Wool fibers/acid red 1	84.8	[41]
Wool fibers/direct red 80	49.5	[41]
74.2% deacetylated chitosan/azonaphthalene-trisulfonate	−2.17	[42]
84.9% deacetylated chitosan/azonaphthalene-trisulfonate	−23.4	[42]
Raw chitin powder/indigo carmine	−40.1	[40]
Raw chitosan powder/indigo carmine	−23.4	[27]
Raw chitosan powder/indigo carmine	−29.2	[43]
Cross-linked chitosan (100 mg mass)/indigo carmine (low dye concentration)	38.2	This work
Cross-linked chitosan (100 mg mass)/indigo carmine (high dye concentration)	110.3	This work
Cross-linked chitosan (300 mg mass)/indigo carmine (low dye concentration)	36.3	This work
Cross-linked chitosan (300 mg mass)/indigo carmine (high dye concentration)	40.1	This work

For the sake of comparison, Table 5 presents comparative values of $\Delta_{ads}H$ for some dye–adsorbent interactions. In general, it has been observed that high exothermic $\Delta_{ads}H$ values (less than $-29\,kJ\,mol^{-1}$) are found for dye adsorptions that occur, mainly, on the surfaces of low-size porous adsorbents. On the other hand, the diffusion of the dye molecules (or ions) into the internal parts of the non-powdered adsorbent materials provokes endothermic and/or very small exothermic values of $\Delta_{ads}H$. So, the wide range of the comparative results of the $\Delta_{ads}H$ in Table 5 (some of them obtained by direct isothermal titration calorimetry) should be seen as evidence that the adsorption thermodynamic values are average results of both diffusional (endothermic) and chemical bonding (exothermic) processes [35]. In addition, the interactive role of the experimental variables, provided in the present work by the factorial design methodology, should also be taking into account to evaluate the changes of the $\Delta_{ads}H$ values.

The positive $\Delta_{ads}S$ values, as well as the very small negative $\Delta_{ads}G$ values found in this work have also been considered as the consequence of the diffusion of the IC dye into the chemical structure of the cross-linked chitosan [20,27,30,34]. In general, high negative $\Delta_{ads}G$ values (less than $-25\,kJ\,mol^{-1}$) are found when adsorption occurs, mainly, on the surfaces of the adsorbents [16,37].

3.3.2. Modeling of the adsorption thermodynamics of IC dye on the cross-linked chitosan

In this work, the adsorption thermodynamics modeling was performed using only the $\Delta_{ads}G$ values, since their values were obtained directly from the equilibrium constants (K). In addition, the values of $\Delta_{ads}H$ and $\Delta_{ads}S$ are similar at 25 and 35 °C, and the factorial design methodology is insensitive to point out differences among them. Thus, the predicted $\Delta_{ads}G$ values, which are presented in lower part of Table 2, were also calculated. Unlike the model presented in Eq. (4), the model for $\Delta_{ads}G$ in Eq. (5) uses all principal and interactive effects observed, since all effects presented statistical significance (Table 3) [23,24]:

$$\Delta_{ads}G = -10.35 + 0.51x_1 + 2.07x_2 - 2.19x_3 + 0.45x_1x_2 - 0.58x_1x_3 + 0.67x_2x_3 + 0.59x_1x_2x_3 \quad (11)$$

where x_1 is the quantity of chitosan, x_2 the concentration and x_3 is the temperature.

It is noted that the adsorption of IC dye, in relation to its energetic point of view, is a complex phenomenon. The concentration of the dye and temperature present more significance in the $\Delta_{ads}G$ values. The principal "mass effect" and almost all interactive effects work to decrease the thermodynamical spontaneity of the adsorption interactions.

4. Conclusions

The results obtained in this study show that the changes proposed in the factorial design study affected the adsorption levels of the IC dye by using cross-linked chitosan.

The results indicated that increasing the chitosan mass from 100 to 300 mg decreases the IC adsorption/mass ratio ($mol\,g^{-1}$) whereas a temperature increase of 25–35 °C increases it. The principal effect of the IC concentration did not show statistical significance. The factorial experiments demonstrate the existence of a significant antagonistic interaction effect between the chitosan mass and temperature. The "concentration effect" was insignificant in relation to the calculated error.

It is noted that the adsorption of IC dye, in relation to its adsorption thermodynamics point of view, is a complex phenomenon. The concentration of the dye and temperature present more significance in the $\Delta_{ads}G$ values. However, the principal "mass effect" and almost all interactive effects work to decrease the thermodynamical spontaneity of the adsorption interactions.

Adsorption works [11,16,38] present $\Delta_{ads}H$ values from -30 to $+158\,kJ\,mol^{-1}$, $\Delta_{ads}G$ from -25 to $+5.0\,kJ\,mol^{-1}$ and $\Delta_{ads}S$ from -100 to $+150\,J\,K^{-1}\,mol^{-1}$. So, the thermodynamic results presented in present work, which are almost all endothermic in nature, are in good agreement with the adsorption studies found in literature. However, only the factorial design methodology can determine the most important principal and interactive factors to change the adsorption thermodynamics at the solid/solution interface.

Acknowledgements

The authors thank the Brazilian National Agency CNPq for fellowships to all authors, and The Primex Ingredients A.S. (Norway/Iceland) for both the free-gift high-quality chitosan sample and the continuous support to our research group.

References

[1] E. Guibal, Interactions of metal ions with chitosan-based sorbents: a review, Sep. Purif. Technol. 38 (2004) 43–74.
[2] G. Crini, Recent developments in polysaccharide-based materials used as adsorbents in wastewater treatment, Prog. Polym. Sci. 30 (2005) 38–70.
[3] A.J. Varma, S.V. Deshpande, J.F. Kennedy, Metal complexation by chitosan and its derivatives: a review, Carbohydr. Polym. 55 (2004) 77–93.
[4] G. Akkaya, I. Uzun, F. Guzel, Kinetics of the adsorption of reactive dyes by chitin, Dyes Pigments 73 (2007) 168–177.
[5] R.A.A. Muzzarelli, Natural Chelating Polymers: Alginic Acid, Chitin and Chitosan, Oxford University Pergamon Press, England, 1973.
[6] E. Guibal, Heterogeneous catalysis on chitosan-based materials: a review, Prog. Polym. Sci. 30 (2005) 71–109.
[7] H.K. No, S.P. Meyers, Application of chitosan for treatment of wastewaters, Rev. Environ. Contam. Toxicol. 163 (2000) 1–28.
[8] W.Q. Sun, G.F. Payne, M.S.G.L. Moas, J.H. Chu, K.K. Wallace, Tyrosinase reaction/chitosan adsorption for removing phenols from wastewater, Biotechnol. Prog. 8 (1992) 179–186.
[9] R.S. Juang, F.C. Wu, R.L. Tseng, Solute adsorption and enzyme immobilization on chitosan beads prepared from shrimp shell wastes, Biores. Technol. 80 (2001) 187–193.
[10] J.M.C.S. Magalhães, A.A.S.C. Machado, Urea potentiometric biosensor based on urease immobilized on chitosan membranes, Talanta 47 (1998) 183–191.
[11] I.S. Lima, C. Airoldi, A thermodynamic investigation on chitosan–divalent cation interactions, Thermochim. Acta 421 (2004) 133–139.
[12] N. Karatepe, Adsorption of a non-ionic dispersant on lignite particle surfaces, Energy Convers. Manage. 44 (2003) 1275–1284.
[13] S. Chegrouche, A. Bensmaili, Removal of Ga(III) from aqueous solution by adsorption on activated bentonite using a factorial design, Water Res. 36 (2002) 2898–2904.

[14] G. Annadurai, R.S. Juang, D.J. Lee, Factorial design analysis for adsorption of dye on activated carbon beads incorporated with calcium alginate, Adv. Environ. Res. 6 (2002) 191–198.
[15] G. Nicholls, B.J. Clark, J.E. Brown, Solid-phase extraction and optimized separation of doxorubicin, epirubicin and their metabolites using reversed-phase high-performance liquid chromatography, J. Pharm. Biomed. Anal. 10 (1992) 949–957.
[16] O.A.C. Monteiro Jr., C. Airoldi, Some thermodynamic data on copper–chitin and copper–chitosan biopolymer interactions, J. Colloid Interf. Sci. 212 (1999) 212–219.
[17] O. Leal, C. Bolévar, C. Ovalles, J.J. Garcia, Y. Espidel, Reversible adsorption of carbon dioxide on amine surface-bonded silica gel, Inorg. Chim. Acta 240 (1995) 183–189.
[18] E.C.N. Lopes, F.S.C. dos Anjos, E.F.S. Vieira, A.R. Cestari, An alternative Avrami equation to evaluate kinetic parameters of the interaction of Hg(II) with thin chitosan membranes, J. Colloid Interf. Sci. 263 (2003) 542–547.
[19] A.R. Cestari, E.F.S. Vieira, E.S. Silva, Interactions of anionic dyes with silica-aminopropyl. 1. A quantitative multivariate analysis of equilibrium adsorption and adsorption Gibbs free energies, J. Colloid Interf. Sci. 297 (2006) 22–30.
[20] A.R. Cestari, E.F.S. Vieira, A.A. Pinto, E.C.N. Lopes, Multistep adsorption of anionic dyes on silica/chitosan hybrid. 1. Comparative kinetic data from liquid- and solid-phase models, J. Colloid Interf. Sci. 292 (2005) 363–372.
[21] E. Guibal, M. Van Vooren, B.A. Dempsey, J. Roussy, A review of the use of chitosan for the removal of particulate and dissolved contaminants, Sep. Sci. Technol. 41 (2006) 2487–2514.
[22] K. Ravikumar, S. Krishnan, S. Ramalingam, K. Balu, Optimization of process variables by the application of response surface methodology for dye removal using a novel adsorbent, Dyes Pigments 72 (2007) 66–74.
[23] G.P.G. Box, J.S. Hunter, W.G. Hunter, Statistics for Experimenters: Design Innovation and Discovery, second ed., John Wiley & Sons, USA, 2005.
[24] R.E. Bruns, I.S. Scarminio, B.B. de Barros Neto, Statistical Design–Chemometrics, Elsevier, Amsterdam, 2006.
[25] A.R. Cestari, E.F.S. Vieira, A.J.P. Nascimento, C. Airoldi, New factorial designs to evaluate chemisorption of divalent metals on aminated silicas, J. Colloid Interf. Sci. 241 (2001) 45–51.
[26] J. Shen, Z. Duvnjak, Adsorption kinetics of cupric and cadmium ions on corncob particles, Process Biochem. 40 (2005) 3446–3454.
[27] F.S.C. dos Anjos, E.F.S. Vieira, A.R. Cestari, Interaction of indigo carmine dye with chitosan evaluated by adsorption and thermochemical data, J. Colloid Interf. Sci. 253 (2002) 243–246.
[28] S.S. Tahir, N. Rauf, Thermodynamic studies of Ni(II) adsorption onto bentonite from aqueous solution, J. Chem. Thermodyn. 35 (2003) 2003–2009.
[29] E. Gimenez-Martin, M. Espinosa-Jiménez, Influence of tannic acid in leacril/rhodamine B system: thermodynamics aspects, Colloids Surf. A 270/271 (2005) 93–101.
[30] R. Goobes, G. Goobes, C.T. Campbell, P.S. Stayton, Thermodynamicvs of statherin adsorption onto hydroxyapatite, Biochemistry 45 (2006) 5576–5586.
[31] Y.-S. Ho, A.E. Ofamaja, Kinetics and thermodynamics of lead ion sorption on palm kernel fibres from aqueous solution, Process Biochem. 40 (2005) 3455–3461.
[32] J. Romero-González, J.R. Peralta-Videa, E. Rodríguez, S.L. Ramirez, J.L. Gardea-Torresdey, Determination of thermodynamic parameters of Cr(VI) adsorption from aqueous solution onto *Agave lechuguilla* biomass, J. Chem. Thermodyn. 37 (2005) 343–347.
[33] A.R. Cestari, C. Airoldi, R.E. Bruns, A fractional factorial design applied to organofunctionalized silicas for adsorption optimization, Colloids Surf. A 117 (1996) 7–13.
[34] A.R. Cestari, E.F.S. Vieira, C.R.S. Mattos, Thermodynamics of the Cu(II) adsorption on thin vanillin-modified chitosan membranes, J. Chem. Thermodyn. 38 (2006) 1092–1099.
[35] A.R. Cestari, E.F.S. Vieira, A.G.P. dos Santos, J.A. Mota, V.P. de Almeida, Adsorption of anionic dyes on chitosan beads. 1. The influence of the chemical structures of dyes and temperature on the adsorption kinetics, J. Colloid Interf. Sci. 280 (2004) 380–386.
[36] J. Wu, H.-Q. Yu, Biosorption of 2,4-dichlorophenol from aqueous solution by *Phanerochaete chrysosporium* biomass: isotherms, kinetics and thermodynamics, J. Hazard. Mater. B 137 (2006) 498–508.
[37] E.F.S. Vieira, A.R. Cestari, J.A. Simoni, C. Airoldi, Thermochemical data for interaction of some primary amines with complexed mercury on mercapto-modified silica gel, Thermochim. Acta 399 (2003) 121–126.
[38] A. Ramesh, D.J. Lee, J.W.C. Wong, Thermodynamic parameters for adsorption equilibrium of heavy metals and dyes from wastewater with low-cost adsorbents, J. Colloid Interf. Sci. 291 (2005) 588–592.
[39] S. Wang, H. Li, L. Xu, Application of zeolite MCM-22 for basic dye removal from wastewater, J. Colloid Interf. Sci. 295 (2006) 71–78.
[40] A.S. Özcan, A. Özcan, Adsorption of acid dyes from aqueous solutions onto acid-activated bentonite, J. Colloid Interf. Sci. 276 (2004) 39–46.
[41] M. Saleem, T. Pirzada, R. Qadeer, Sorption of some azo-dyes on wool fiber from aqueous solutions, Colloids Surf. A 260 (2005) 183–188.
[42] T.K. Saha, S. Karmaker, H. Ichikawa, Y. Fukumori, Mechanisms and kinetics of trisodium 2-hydroxy-1,1′-azonaphthalene-3,4′,6-trisulfonate adsorption onto chitosan, J. Colloid Interf. Sci. 286 (2005) 433–439.
[43] A.G.S. Prado, J.D. Torres, E.A. Faria, S.C.L. Dias, Comparative adsorption studies of indigo carmine dye on chitin and chitosan, J. Colloid Interf. Sci. 277 (2004) 43–47.